Nonparametric Statistical Snake Based on the Minimum Stochastic Complexity

Pascal Martin, Philippe Réfrégier, Frédéric Galland, and Frédéric Guérault

***Abstract*—We propose a nonparametric statistical snake technique that is based on the minimization of the stochastic complexity (minimum description length principle). The probability distributions of the gray levels in the different regions of the image are described with step functions with parameters that are estimated. The segmentation is thus obtained by minimizing a criterion that does not include any parameter to be tuned by the user. We illustrate the robustness of this technique on various types of images with level set and polygonal contour models. The efficiency of this approach is also analyzed in comparison with parametric statistical techniques.**

***Index Terms*—Image segmentation, level set, minimum description length principle, snakes, stochastic complexity.**

I. Introduction

An IMPORTANT goal of computational vision and image processing is to automatically recover the shape of objects from various types of images. Over the years, many approaches have been developed to reach this goal. In this paper, we focus on the segmentation of objects using active contours (snakes).

The first snakes [1] were driven by the minimization of a function in order to move them towards desired features, usually edges. These approaches are edge based in the sense that the information used is strictly along the boundary. They are well adapted to a certain class of problems, but they can fail in the presence of strong noise, although several improvements and reformulations have been proposed to overcome these limitations [2], [3] (and references therein). Another strategy consists in considering not only the edges, but also the inner and the outer regions defined by the active contour [4]–[8].

In the region-based approaches, the contour is deformed to minimize a criterion that is the sum of two terms [9]–[12]: the external energy, that is based on the gray levels of the image and on a statistical model, and the internal energy, that allows one to regularize the contour. It has been shown that the minimization of the stochastic complexity [13] leads to a satisfying tradeoff between these two energies for various types of contour models (spline [14], polygonal [15], level set [16]). The resulting snakes present clear optimal properties in the context of statistical estimation theory if the *a priori* gray-level probability distribution (GLPD) model is well adapted to the data.

The GLPD models that belong to the exponential family [10] allow one to deal with many applications (radar images, low photon flux, ...). Nevertheless, such parametric models may fail to provide a fair description of the GLPD in some practical cases and different approaches were developed to overcome these limitations. In [17], the authors proposed to estimate the GLPD on the whole image with a Gaussian mixture such that each element of the mixture corresponds to a region. Although this approach is interesting and provides good results on different types of images, we will see that it is preferable to estimate the GLPD in each region. In [18], a supervised method is proposed for texture segmentation tasks. This approach requires training which is an important difference with the technique proposed in this paper. In [19] and [20], the authors proposed a nonparametric statistical approach based on the estimation of the GLPD with Parzen windows [21]. A level set implementation in which the variance σ_P of the Gaussian kernel is automatically estimated has also been developed [22]. However, in these approaches [19], [20], [22] the criterion to optimize contains a tuning parameter in order to balance the contribution of the internal and of the external energy.

We propose in this paper a segmentation technique that is based on the minimization of a criterion without tuning parameter and that is not dedicated to a particular probability distribution family. For that purpose, the GLPD of the object and of the background are described with step functions with parameters and number of steps estimated from the image in hand. This is an important difference to the previous cited nonparametric statistical snake techniques and to our knowledge, this is the first demonstration of snake segmentation based on a criterion without tuning parameter and that is not dedicated to a particular GLPD. It will be studied when the results are equivalent to the ones obtained when a parametric statistical model adapted to the fluctuations present in the image is used. Furthemore, we shall also demonstrate the stronger robustness of the technique proposed in this paper.

The general model of the stochastic complexity is presented in Section II. Experimental results are provided in Section III on synthetic and real images.

II. Minimum Stochastic Complexity Approach

In this section, the stochastic complexity that corresponds to the criterion that will be minimized in order to segment the image with snake models is defined.

Manuscript received March 7, 2005; revised November 22, 2005. The associate editor coordinating the review of this manuscript and approving it for publication was Prof. Vincent Caselles.

P. Martin is with the Physics and Image Processing Group, Fresnel Institute UMR CNRS 6133, Ecole Généraliste d'Ingénieurs de Marseille, Domaine Universitaire de St Jérôme, 13397 Marseille Cedex 20, France, and also with the Simag Développement, 13016 Marseille, France (e-mail: pascal.martin@fresnel.fr).

P. Réfrégier and F. Galland are with the Physics and Image Processing Group, Fresnel Institute UMR CNRS 6133, Ecole Généraliste d'Ingénieurs de Marseille, Domaine Universitaire de St Jérôme, 13397 Marseille Cedex 20, France (e-mail: philippe.refregier@fresnel.fr; frederic.galland@fresnel.fr).

F. Guérault is with Simag Développement, 13016 Marseille, France (e-mail: frederic.guerault@simag.fr).

Digital Object Identifier 10.1109/TIP.2006.877317

1057-7149/$20.00 © 2006 IEEE

Authorized licensed use limited to: Pierre Borgnat. Downloaded on February 27, 2009 at 04:51 from IEEE Xplore. Restrictions apply.

A. General Model

Let $\mathbf{s} = \{s(x,y)|(x,y) \in [1,N_x] \times [1,N_y]\}$ denote the image to segment with $N_x \times N_y$ pixels and with gray levels quantized on Q levels. One thus has $s \in [1,Q]$ with $Q \in \mathbb{N}$ (for example, $Q = 256$). One assumes that the image is composed of R regions Ω_u with $u = 1,\ldots,R$ (not necessarily simply connected). The number of pixels of Ω_u will be noted N_u. The gray levels of Ω_u are assumed to be spatially uncorrelated and independently distributed with GLPD P^u.

With statistical region-based snakes, the criterion that has to be optimized in order to find the final contour Γ can be obtained by determining the stochastic complexity of the image [14]–[16]. With this approach, one has to determine the sum of the number of bits needed for the description of the data and for the description of the model of the data [13]. Since the model of the data includes the contour model and the GLPD P^u, the stochastic complexity can be written as the sum of three terms

$$\Delta = \Delta_S + \Delta_P + \Delta_C \tag{1}$$

where Δ_S is the number of bits needed to code the gray levels of the image with both the contour Γ and the GLPDs $P^1,\ldots,P^R$ fixed, Δ_P is the number of bits needed to code the GLPDs and Δ_C is the number of bits needed to code the contour Γ. In the following, these quantities will be measured in nats (i.e., natural logarithm will be considered). We detail in the following the particular expression of these different terms.

B. Gray Level Coding

The number of nats Δ_S needed to describe the gray levels of $\mathbf{s}$ with given GLPDs $P^1,\ldots,P^R$ is simply equal to

$$\Delta_S = -\sum_{u=1}^{R} \sum_{(x,y)\in\Omega_u} \log\left(P^u[s(x,y)]\right) \tag{2}$$

since in Ω_u, the number of nats needed to code the value $s(x,y)$ with an entropic code [23] is $-\log\left(P^u[s(x,y)]\right)$.

The choice of the GLPD estimation technique we have done is based on two constraints. The first one is to get similar segmentation performances to the ones obtained with techniques based on parametric statistical models adapted to the gray-level fluctuations. The second constraint is to develop a technique which can lead to low computational time. For that purpose, we propose to estimate the GLPD in each region Ω_u with an irregular step function $P_q^u(s)$ with q steps (Fig. 1)

$$P_q^u(s) = \sum_{j=1}^{q} p_u(j) R_j(s) \tag{3}$$

where $R_j(s) = 1$ if $s \in [a_j, a_{j+1}[$ and $R_j(s) = 0$ otherwise, with $a_j \in [1,Q]$, $a_1 = 1$, $a_{q+1} = Q+1$ and $a_j > a_i$ if $j > i$ and where the a_j are identical for each distribution P_q^u. One thus has $P_q^u(s) = p_u(j)$ if $s \in [a_j, a_{j+1}[$. This is a general model that can describe any distribution of random variable quantized on Q levels. In particular, we shall show on real images that this approach allows one to perform SAR image segmentation

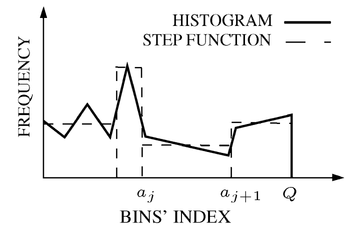

Fig. 1. Illustration of the estimation of the GLPD. Solid line: histogram. Dotted line: step function.

for which the fluctuations are multiplicative. Indeed, once the noise is present in each region of the image, the way the random gray levels have been generated is no more important and only the difference between the histograms of the different regions is relevant.

In each region Ω_u and for given values of the a_j, the maximum likelihood estimation $\widehat{p}_u(j)$ of the $p_u(j)$ is

$$\widehat{p}_u(j) = \frac{1}{b_j N_u} \sum_{(x,y)\in\Omega_u} R_j(s(x,y)) = \frac{N_u(j)}{b_j N_u} \tag{4}$$

where $b_j = a_{j+1} - a_j$ and where $N_u(j)$ is the number of pixels in Ω_u such as $s \in [a_j, a_{j+1}[$. One thus gets

$$\Delta_S = -\sum_{u=1}^{R} \sum_{j=1}^{q} N_u(j) \log\left[\frac{N_u(j)}{b_j N_u}\right]. \tag{5}$$

At this level of the analysis, only the parameters a_j, and as a consequence the number of steps q, of the steps functions are undetermined. They will be estimated by minimizing the global stochastic complexity which needs that we detail the expression of Δ_P and Δ_C.

C. Gray-Level Probability Distribution Coding

In order to determine Δ_P, one has to evaluate the number of nats necessary to code the different distributions P^u. From (3) and (4), it is clear that we need to code the $\widehat{p}_u(j)$ for $j = 1,\ldots,q-1$ (since $\sum_{j=1}^{q} b_j \widehat{p}_u(j) = 1$). We propose to demonstrate in the following that the simple approximation provided by the application of the minimum description length principle [13], [24] is sufficient. With this approximation, coding $\widehat{p}_u(j)$ needs $\log(\sqrt{N_u})$ nats. Furthermore, one also needs to code $q-1$ values b_j (since $\sum_{j=1}^{q} b_j = Q$). We consider that coding the value b_j requires approximately $\log(1+b_j)$ nats since $b_j = 1$ needs to be coded with at least one bit. Since the values b_j are equal in each region, one gets

$$\Delta_P = \sum_{u=1}^{R} (q-1) \log\left[\sqrt{N_u}\right] + \sum_{j=1}^{q-1} \log(1+b_j). \tag{6}$$

D. Shape Descriptor Coding

From a practical point of view, the term Δ_C leads to a regularization of the contour [14]–[16]. Let us recall its expression for the particular contour models we consider in this paper.

Authorized licensed use limited to: Pierre Borgnat. Downloaded on February 27, 2009 at 04:51 from IEEE Xplore. Restrictions apply.

For level set snakes, the contour is considered to be the zero level set of a function $z=\phi(x,y)$ where $\phi(x,y)$ is the euclidian distance to the contour $\Gamma=\{(x,y)|\phi(x,y)=0\}$ [25]–[30], [12], [31]. This contour model allows to segment the image in two regions (i.e., $R=2$) not necessarily simply connected. For such contour models, the number of nats required to code the contour can be approximated by [16]

$$\Delta_C^{LS}=\log(8)|\Gamma| \quad (7)$$

where $|\Gamma|$ is the length in pixel units of the contour.

For an unique and simply connected object to segment in the image, it can be advantageous to consider polygonal contour models [10], [15]. It has been shown [15] that the minimization of the stochastic complexity can lead to efficient technique without tuning parameter in the optimized criterion when the gray-level fluctuations follow a parametric probability density function (pdf) that belongs to the exponential family and that is adapted to the fluctuations present in the image. This approach has been generalized to a multiregion snake in [32] and the number of nats needed to code such a multiregion polygonal contour can be approximated by

$$\Delta_C^P=n\log N+(n+1)\log p+p\left[2\log(2e)+\log(\widehat{m}_x\,\widehat{m}_y)\right] \quad (8)$$

where $\widehat{m}_x$ (respectively, $\widehat{m}_y$) is the mean value of horizontal (respectively, vertical) distances between adjacent nodes, n is the number of Eulerian graphs of the multiregion polygonal snake, and p its number of segments.

Of course, this approach could be generalized to other contour models such as spline descriptors for example [14] or multiregion level-set techniques [33], [34]. However, for sake of simplicity, this paper focuses on level-set and polygonal snakes for the segmentation in two regions. The more general case of multiregion polygonal snakes with a known but arbitrary number of regions will be also considered as an illustration.

E. Optimization Strategy

The segmentation of the image is obtained by minimizing the stochastic complexity Δ. This criterion depends on the contour Γ (i.e., the parameter of interest) and on the q parameters a_j that are introduced for the description of the distribution probabilities P^u. These parameters (Γ, $a_1,\ldots,a_q$ and q of the step function) can be obtained by minimizing Δ. For that purpose, Γ is estimated by minimizing Δ with fixed a_j. Then, the parameters a_j and q are determined by minimizing Δ for the given value of Γ, and the process is iterated if necessary.

1) Level Set Contour Estimation: In this subsection, the implementation of the minimization along Γ is described. This technique is standard in level-set implementation, thus we refer to published works for further details [26], [31], [16]. The equation evolution is given [26] by the partial differential equation $\partial\phi(x,y)/\partial t=F(s(x,y))|\nabla\phi(x,y)|$. Considering the discrete expression, one obtains

$$\phi_{t+1}(x,y)-\phi_t(x,y)=\varepsilon\times F(s(x,y))\times|\nabla\phi_t(x,y)| \quad (9)$$

where ε is a small parameter, ϕ_t is the Euclidian distance function to the contour Γ obtained at step t, and $|x|$ is the modulus of x. The force term $F(s(x,y))$ that drives the deformation of the distance function at pixel of coordinates (x,y) is given by $F(s(x,y))=\partial\Delta/\partial\Gamma$. According to (1), it is the sum of 3 terms $F_S(s(x,y))=\partial\Delta_S/\partial\Gamma$, $F_P(s(x,y))=\partial\Delta_P/\partial\Gamma$ and $F_C^{LS}(s(x,y))=\partial\Delta_C^{LS}/\partial\Gamma$.

In order to simplify the analysis, it is possible to neglect the term $F_P(s(x,y))$. Indeed, this approximation is equivalent to consider $(q-1)\log\left[\sqrt{N}\right]$ instead of $(q-1)\log\left[\sqrt{N_u}\right]$ in (6) which is also an acceptable approximation of Δ_P. It was established in [16], that $F_C^{LS}(s(x,y))=-\log(8)\mathcal{K}$ where $\mathcal{K}$ is the curvature defined by $\mathcal{K}=div\,(\nabla\phi/|\nabla\phi|)$. Using the results in [16], one can show that the expression for $F_S(s(x,y))$ is as shown in (10), at the bottom of the page, where $\mathrm{H}(z)=-z\log(z)$ and $n_u(j)=N_u(j)/N_u$. The expression of $F_S(s(x,y))$ is obtained by considering small deformation of the contour Γ and is thus valid only close to Γ. This approximation is consistent with a narrowband implementation [35], which is also interesting in order to reduce the computational time.

2) Polygonal Contour Estimation: The optimal shape is obtained by simultaneously determining the value k of the number of nodes of the polygonal snake and their locations. Following [32], [15], this double optimization problem is addressed through a two-step procedure.

In the first step, after convergence obtained by minimizing Δ with a given value k, this number of nodes is increased so that the distance between two consecutive nodes cannot exceed a given value. This process is initialized with a low k value and stopped when the distance between adjacent nodes is typically equal to two or four pixels.

The second step is a complexity-reduction technique and consists in removing the node leading to the greatest decrease of Δ and the process is iterated until the minimum of Δ has been obtained.

3) GLPD Estimation: The parameters a_j and q are estimated by minimizing Δ for a given estimation of the contour Γ. Since the estimation starts with the general distribution model for which $q=Q$ and $a_j=j$, the estimation of the a_j can be obtained by merging the couple of steps $[a_{j-1},a_j[$ and $[a_j,a_{j+1}[$

$$F_S(s(x,y))=\sum_{j=1}^{q}\left\{\mathrm{H}(n_1(j))-\mathrm{H}(n_2(j))+\frac{\partial\mathrm{H}(n_1(j))}{\partial n_1(j)}\left[R_j(s(x,y))-n_1(j)\right]-\frac{\partial\mathrm{H}(n_2(j))}{\partial n_2(j)}\left[R_j(s(x,y))-n_2(j)\right]\right\} \quad (10)$$

Authorized licensed use limited to: Pierre Borgnat. Downloaded on February 27, 2009 at 04:51 from IEEE Xplore. Restrictions apply.

that leads to the greatest decrease of Δ among all the possible fusions. The fusion of the two selected steps provides a new step $[a_{j-1}, a_{j+1}[$ and the probability of observing a value s in this interval becomes $b_{j-1}\widehat{p}_u(j-1) + b_j\widehat{p}_u(j)$. The process is iterated and the step function that minimizes Δ is selected.

4) Global Optimization Strategy: After each step fusion, a new convergence of the contour can be implemented from the contour obtained before this fusion in order to get a better estimation of the stochastic complexity of the image. Since this full-iterative strategy can be time consuming, one will compare the obtained results with a simplest approach, denominated three-stage strategy in the following. With this approach (illustrated in Fig. 2), an initial convergence is performed considering step functions with $q = 20$ such that each step is of equal length. Then, no convergence of the contour is performed between fusion of steps of the probability distribution (starting from $q = Q$). However, when the a_j and q have been estimated, a final convergence of the contour is performed from the contour obtained before the step fusions.

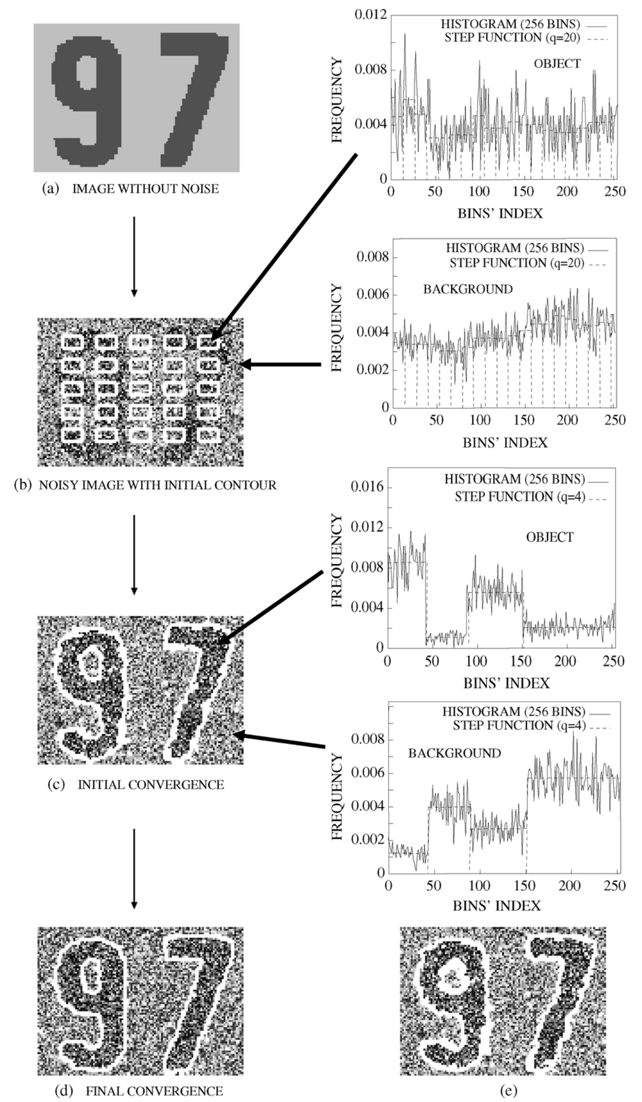

Fig. 2. Illustration of the three-stage strategy. (a) Synthetic image without noise (115 × 83 pixels). (b) Noisy version quantized with $Q = 256$ levels and with initial contour. One can see the histograms and the step functions of parameter $q = 20$ associated to the object and the background of the image (b). (c) Initial convergence performed considering step functions of parameter $q = 20$. One can see the histograms associated to the image (c) and the step functions with number of steps estimated ($q = 4$) after the initial convergence. (d) Final convergence performed from the contour obtained at the end of the initial convergence and with the estimated GLPDs. (e) Final contour obtained considering $q = Q = 256$.

III. Experimental Results

This section provides an evaluation of our method. Synthetic images are first considered since they allow one to get a precise determination of the number of misclassified pixels (NMP). Real images are also considered to shed light in the performance in a practical case. These results demonstrate that the simple proposed approaches for estimating the GLPD and for the optimization strategy provide good results and lead to a simple and fast segmentation technique.

A. Influence of the Optimization Strategy

In order to compare the two optimization strategies introduced in Section II-E, the average number of misclassified pixels (ANMP) after segmentation is computed. The synthetic images considered are noisy versions of the image Fig. 2(a) perturbed with Gaussian, Gamma and Poisson noises for different values of the contrast between the two regions in the image. This contrast can be measured with the Kullback-Leibler divergence [23] or the Bhattacharyya [23] distance between the distributions of the background and target gray levels. However, it has been shown [36] that, for small targets, the Bhattacharyya distance is a better measure of contrast. In particular, different noisy configurations with the same value of $\mathcal{B}$ lead to similar values of the ANMP for different types of noises for polygonal snakes [36] and for level-set snakes with parametric pdf models [16]. In the continuous case, the Bhattacharyya distance between pdf P^t and P^b reads

$$\mathcal{B} = -\log \int \sqrt{P^t(z)P^b(z)}dz \tag{11}$$

while in the discrete case it is $\mathcal{B} = -\log \sum_z \sqrt{P^t(z)P^b(z)}$. The NMP after a segmentation is determined from the final contour by counting the number of pixels that belong to the true target shape but lie outside the contour Γ, and those that belong to the true background but lie inside the contour Γ. In the following, the values of the NMP will be normalized by the number of pixels in the true shape of the target.

For the level-set snake implementation, one can see in Fig. 3 that the two optimization strategies lead to equivalent segmentation results. This result has been confirmed with different experiments and with polygonal snake implementations. The three-stage strategy is much faster (a few tens of seconds instead of many minutes). For example, the image Fig. 2(b) has been segmented in 12 min with the full-iterative strategy and only in 41

Authorized licensed use limited to: Pierre Borgnat. Downloaded on February 27, 2009 at 04:51 from IEEE Xplore. Restrictions apply.

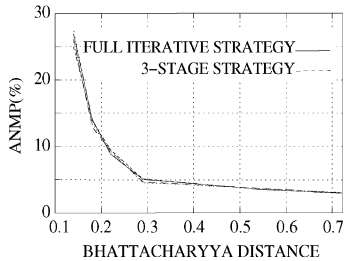

Fig. 3. ANMP as a function of the Bhattacharyya distance $\mathcal{B}$ for segmentation results obtained with the level-set snake and the two strategies on the image Fig. 2(a) pertubed with Gaussian, Gamma and Poisson noises. Each ANMP has been estimated on 20 noise realizations.

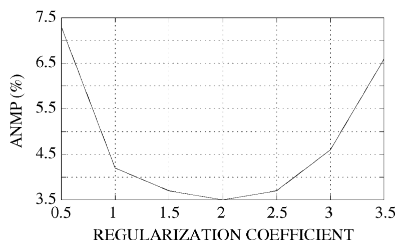

Fig. 4. ANMP as a function of λ obtained with the level-set snake implemented with the three-stage strategy on the image Fig. 2(a) perturbed with Poisson noise ($\mathcal{B} = 0.55$). Each ANMP has been estimated on 20 noise realizations. Similar results are obtained with other noise distributions such as Gaussian or Gamma.

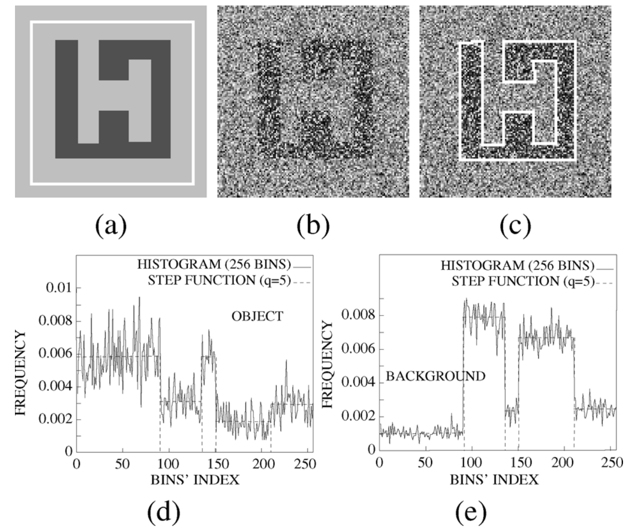

Fig. 5. (a) Image (128×128 pixels) without noise and with initial contour. (b) Noisy version of image (a). (c) Polygonal contour estimated with the three-stage strategy. (d), (e) Histograms (solid line) and estimated GLPDs (dotted line) of the object and background.

s with the three-stage strategy. So, this faster strategy will only be considered in the following.

B. Evaluation of the Contour Regularity

We show in this subsection that the minimization of the stochastic complexity leads to contour with the appropriate regularity. For that purpose, a successive analyzis of the level-set and of the polygonal snakes adapted to images with two regions is performed.

According to Section II-D, the stochastic complexity for level-set snakes leads to $\Delta_C^{LS} = \lambda|\Gamma|$ with $\lambda = \log(8)$. Fig. 4 establishes this value $\lambda_{opt} = \log(8) \simeq 2$ is indeed optimal if different segmentations are performed with different values of λ.

A segmentation result obtained with a polygonal contour model and the three-stage strategy on an image quantized with $Q = 256$ levels is shown in Fig. 5. The noisy image in Fig. 5(b) was generated with a polygon with 16 nodes and an object and a background gray-level distributions generated with step functions with $q = 5$ steps. The histograms and the estimated distributions are shown in Fig. 5(d) and in Fig. 5(e). The segmentation result is shown in Fig. 5(c) and corresponds to an estimated polygonal snake with 16 nodes (i.e., equal to the true value).

C. Influence of the GLPDs Modelization

In order to analyze the relevance of estimating the GLPDs with step functions whose parameters q and a_j are estimated by minimizing the stochastic complexity, segmentation results obtained with the level-set snake on a noisy image quantized with $Q = 256$ levels are shown in Fig. 2. The noisy image has been generated with an object and a background gray-level distributions that correspond to step functions with $q = 4$.

From Fig. 2(c) and Fig. 2(e), it is clear that estimating the GLPDs either with $q = 20$ (initial convergence of the three-stage strategy) or with its histograms leads to significant fluctuations of the estimated contours. (i.e., when q is fixed to 256 and is not estimated). When the three-stage strategy is implemented the estimated value of q is equal to 4 (i.e., is equal to the true value) and the corresponding segmentation result is greatly improved—see Fig. 2(d).

We now propose to show that estimating the parameters a_j and q of the GLPD on the whole image instead of implementing the three-stage approach developed above may not allow one to get satisfactory segmentation results. In particular, This result illustrates the improvement of the proposed approach in comparison to the one developed in [17], that consists of performing the estimation of the gray-level pdf of the object and background regions on the whole image before the segmentation. For that purpose, the parameters a_j and q of the GLPD are estimated on the whole image by minimizing the following stochastic complexity [24]

$$\Delta^I(\mathbf{s}:) = -\sum_{j=1}^{q} N(j)\log\left[\frac{N(j)}{b_j N}\right] + (q-1)\log\left[\sqrt{N}\right] + \sum_{j=1}^{q-1}\log(1+b_j) \quad (12)$$

where $N(j)$ is the number of pixels in the image such that $s \in [a_j, a_{j+1}[$. This approach is analogous to the one developed in Section II-C but with a unique region for the GLPD estimation.

The GLPD of the whole image shown in Fig. 2(b) is presented in Fig. 6 and its estimation with a step function is represented in dotted line. The minimization of (12) lead to $q = 1$

Authorized licensed use limited to: Pierre Borgnat. Downloaded on February 27, 2009 at 04:51 from IEEE Xplore. Restrictions apply.

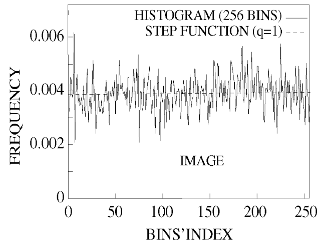

Fig. 6. Solid line: histogram. Dotted line: estimated GLPD obtained on the whole image of Fig. 2.

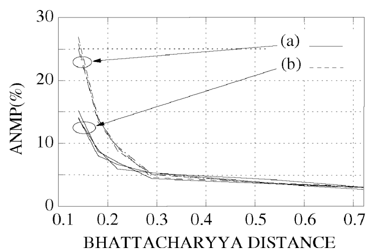

Fig. 7. ANMP as a function of the Bhattacharyya distance $\mathcal{B}$ for segmentation results obtained with the parametric statistical approach and the proposed technique with the three-stage strategy on the image of Fig. 2(a) with Gaussian, Gamma and Poisson GLPDs. Each ANMP has been estimated on 20 noise realizations and the segmentation is performed with the level-set snake. (a) Nonparametric statistical approach. (b) Parametric statistical approach.

and does not allow one to separate the object and the background whereas good results are obtained [Fig. 2(d)] with the three-stage strategy.

D. Comparison With Parametric Statistical Approach

When the gray levels of the different regions of the image are distributed with pdf that belong to the exponential family, efficient snake based techniques that relie on the minimization of the stochastic complexity [15], [16] can be developed. Our aim in this subsection is to compare the segmentation results obtained with these parametric statistical approaches [15], [16] to the ones obtained with the proposed nonparametric statistical approach of this paper when a level-set implementation is used.

First, let us consider the case of gray levels in the images that are distributed according to the exponential family. For that purpose, one considers different noisy versions of the image of Fig. 2(a) with Gaussian, Gamma, or Poisson distributions. The evolution of the ANMP as a function of the Bhattacharyya distance $\mathcal{B}$ is shown in Fig. 7. Twenty realizations of the scene were generated for each noise model and for different values of $\mathcal{B}$. The obtained images have been segmented either with the parametric statistical approach or with the three-stage strategy. Fig. 7 illustrates that the performances of the proposed approach are similar for the three types of pdf. Moreover, the parametric statistical approach and the nonparametric statistical approach of this paper lead to similar values of the ANMP when $\mathcal{B} \geq 0.3$. If $\mathcal{B} < 0.3$ the proposed approach provides worse results than the parametric statistical approach that also leads to degraded performance.

Clearly, our nonparametric method does not rely on a given model. This is a major advantage over parametric methods that can produce very bad results if the parametric model does not correspond to the noise in the data. Fig. 8 illustrates this effect

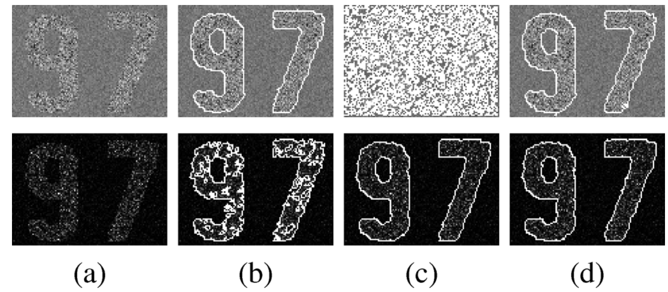

Fig. 8. (a) Synthetic images (115 × 83 pixels) perturbed with Gaussian (first line) and Gamma (second line) noises with $\mathcal{B} = 0.29$. Segmentation results obtained with (b) Gaussian and (c) Gamma models for the GLPDs and (d) the proposed approach with the three-stage strategy. The level-set snake has been used and the initial contour is the one of Fig. 2(b).

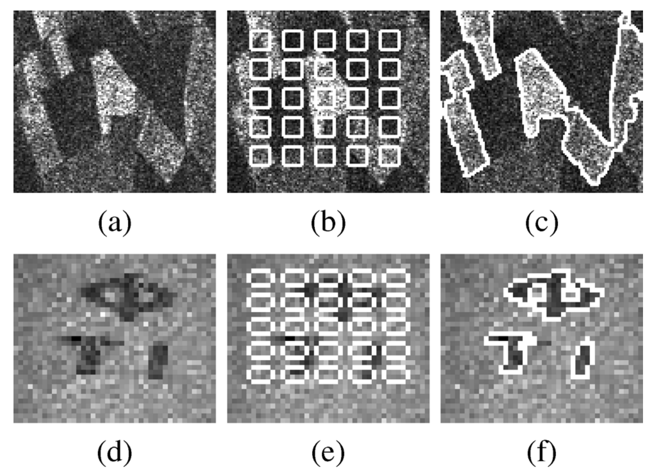

Fig. 9. (a) SAR image (120 × 108 pixels) of an agricultural area obtained by the ERS-1 satellite (distributed by the ESA and provided by the CNES). (b) Initial contour. (c) Final contour obtained with the three-stage strategy (computation time: 15 s). (d) Scene illuminated by a laser (41 × 34 pixels). (e) Initial contour. (f) Final contour obtained with the three-stage strategy (computation time: 0.4 s). The level-set snake has been used. For a better visualization, the contrast of the images has been increased.

and compares both approach on a synthetic image with different noise distributions.

In conclusion, the nonparametric approach proposed in this paper with the three-stage strategy leads to satisfactory result in comparison to the ones obtained with a parametric model adapted to the gray-level fluctuations, but with a stronger robustness.

E. Real Images

We propose to show in this subsection segmentation examples obtained with the proposed nonparametric statistical technique and the three-stage strategy on different types of real images. The segmentations have been performed with a PC Intel Xeon 2.8 GHZ (Linux 2.4, gcc 2.96) with 900 Mo of RAM and the computational times are provided in the captions of the figures.

We first show results obtained with the level-set implementation. In Fig. 9(c), the final contour obtained on a real SAR image corrupted with speckle noise is represented. The segmentation result on a laser illuminated image perturbed with speckle noise [37] is shown in Fig. 9(f). In Fig. 10, one can see the segmentation result on a video textured image. We show in Fig. 10(a)

Authorized licensed use limited to: Pierre Borgnat. Downloaded on February 27, 2009 at 04:51 from IEEE Xplore. Restrictions apply.

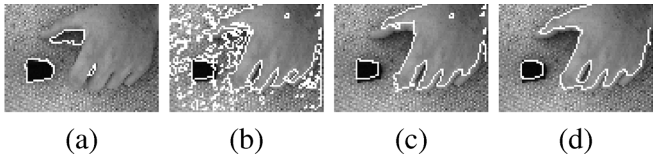

Fig. 10. Segmentation of an image (86×60 pixels) acquired with a CCD camera. (a) Segmentation result obtained with the proposed nonparametric technique with the three-stage strategy. Results of the segmentation on a preprocessed version of (a) obtained with: (b) a Gaussian model for the GLPDs, (c) a Gamma model for the GLPDs, and (d) the proposed nonparametric statistical technique with the three-stage strategy (computation time: 4 s). The same kind of initialization as in Fig. 9(b) has been used for the level-set snake.

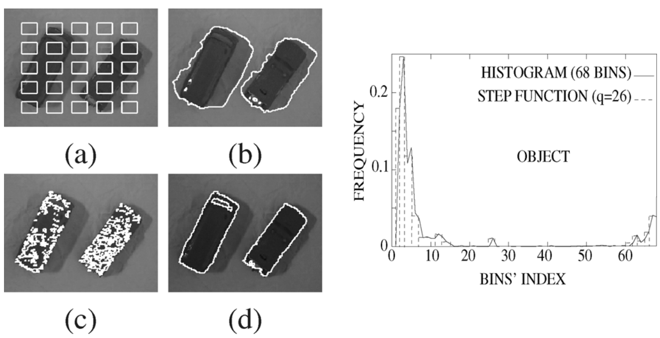

Fig. 11. Example of level snake segmentation. (a) RGB image with 227×174 pixels and initial contour. (b) Segmentation result obtained on the gray-level image with a Gaussian model for the GLPDs. Segmentation obtained on the hue component in the HSV representation with: (c) a Gaussian model, (d) the proposed nonparametric statistical technique (computation time: 21.4 s). (e) Histogram (solid line) and estimated GLPDs (dotted line) of the object in the hue component.

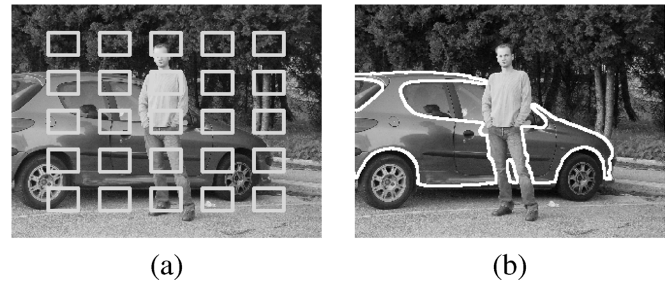

Fig. 12. (a) RGB image acquired with a CCD camera (320×240 pixels) and initial contour. (b) Segmentation results obtained on the hue component in HSV representation with the proposed nonparametric statistical technique with the three-stage strategy and the level-set snake implementation (computation time: 75 s).

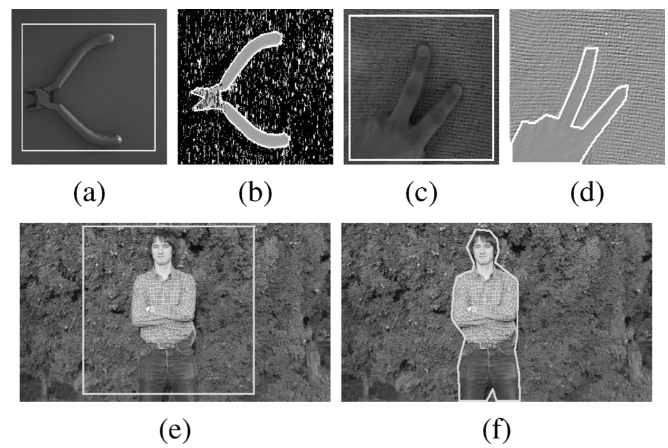

Fig. 13. Examples of segmentation obtained with the polygonal snake. (a) RGB image with 214×278 pixels and initial contour. (b) Final contour displayed on the hue component of the HSV representation (computation time : 8.8 s). (c) Gray-level image with 159×138 pixels and initial contour. (d) Final contour obtained on a preprocessed version of (c) (computation time : 2.2 s). For a better visualization, the contrast of the images has been increased. (e) RGB image with 492×283 pixels and initial contour. (f) Segmentation results obtained on the hue component H in HSV representation (computation time: 10 s).

the result obtained when the technique is applied on the image. One can see in that case that the technique is inefficient since the presence of shadows in the image leads to nonhomogenous regions. However, if one considers the new image $\mathbf{f}$ defined by $f(x,y) = |F_V * s(x,y)|^2 + |F_H * s(x,y)|^2$, where F_V and F_H are the Roberts filters [38] defined with a 3×3 pixel neighborhoods and $*$ is the convolution operator, one obtains an image with two regions more homogenous. Indeed, the gradient operator allows one to suppress linear continuous variation of the gray levels. The segmentation result on this preprocessed image with the proposed technique is shown in Fig. 10(d) and one can see in Fig. 10(b) and (c) that parametric statistical approaches do not lead to satisfactory segmentations. Analogous result on a RGB image acquired with a CCD camera is shown in Fig. 11 where the considered preprocessing now simply consists in extracting the hue component in the HSV representation [39]. Another segmentation example obtained on the hue component of a RGB image is shown in Fig. 12.

We show in Fig. 13 segmentation results obtained with a polygonal snake adapted to two regions. Results on the hue component in the HSV representation are shown in Fig. 13(b) and (f). In Fig. 13(d), the segmentation has been obtained on a gray-level image which has been preprocessed in order to obtain a new image $\mathbf{g}$, defined by $g(x,y) = s(x,y) - s(x+1,y+1)$, in which the different regions are more homogenous.

We show in Fig. 14 segmentation results obtained with a polygonal snake adapted to three regions on RGB images. Segmentation results have respectively been obtained on the hue component in the HSV representation in Fig. 14(b) and on the saturation component in the HSV representation in Fig. 14(d). The image in Fig. 14(c) is extracted from the Berkeley Dataset of natural images [40].

These results show that the proposed approach allows one to deal with very different types of images.

IV. Conclusion

We have proposed a nonparametric statistical snake based on the minimization of the stochastic complexity and where the gray-level distributions of the object and of the background are approximated by step functions whose parameters are estimated during the segmentation process. This approach leads to minimize a criterion without free parameter to be tuned by the user and can be implemented with different contour descriptors such as level-set snake or polygonal contour model. We have illustrated the results on SAR, video (color), and textured images. Moreover, up to low contrast values, we have shown that when the gray-level pdf of the image belong to the exponential family, the proposed approach provide segmentation results equivalent to those obtained with a parametric statistical approach. Of course, the main advantage of the proposed nonparametric statistical technique is its robustness since it adapts to

Authorized licensed use limited to: Pierre Borgnat. Downloaded on February 27, 2009 at 04:51 from IEEE Xplore. Restrictions apply.

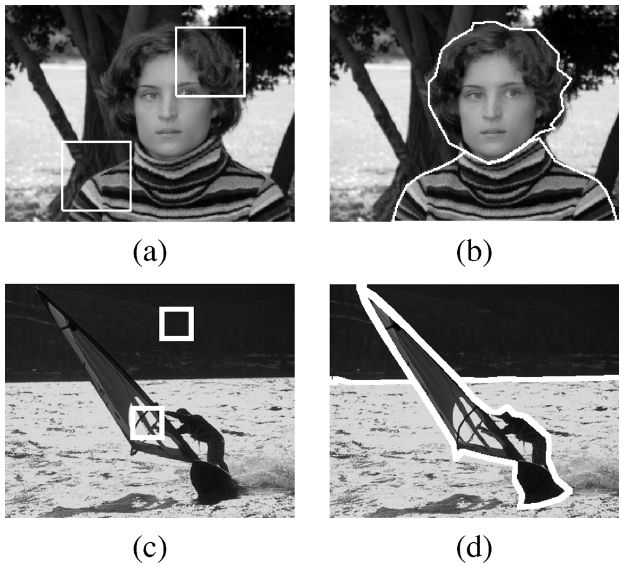

Fig. 14. (a), (c) RGB images (192×156 and 321×398 pixels) and initial contours. Segmentation results obtained with the proposed nonparametric statistical polygonal technique adapted to three regions with the three-stage strategy: (b) on the hue component in HSV representation (computation time: 5.1 s) and (d) on the saturation component in HSV representation (computation time : 11.4 s).

the fluctuation distributions of the gray levels without requiring *a priori* information.

There exists different perspectives to this work. It would be interesting to generalize this technique to other multiregion approaches based for example on level-set techniques. Taking into account possible spatial correlations is also a challenging problem.

Acknowledgment

The authors are grateful to Conseil Régional PACA for taking part in the financing of the Ph.D. degree of P. Martin.

References

[1] M. Kass, A. Witkin, and D. Terzopoulos, "Snakes: Active contour models," *Int. J. Comput. Vis.*, vol. 1, pp. 321–331, 1988.
[2] G. I. Chiou and J. N. Hwang, "A neural network-based stochastic active contour model (nns-snake) for contour finding of distinct features," *IEEE Trans. Image Process.*, vol. 4, no. 10, pp. 1407–1416, Oct. 1995.
[3] C. Xu and J. L. Prince, "Snakes, shapes, and gradient vector flow," *IEEE Trans. Image Process.*, vol. 7, no. 3, pp. 359–369, Mar. 1998.
[4] G. Storvik, "A Bayesian approach to dynamic contours through stochastic sampling and simulated annealing," *IEEE Trans. Pattern Anal. Mach. Intell.*, vol. 16, no. 10, pp. 976–986, Oct. 1994.
[5] A. K. Jain, Y. Zhong, and S. Lakshmanan, "Object matching using deformable template," *IEEE Trans. Pattern Anal. Mach. Intell.*, vol. 18, no. 3, pp. 268–278, Mar. 1996.
[6] J. Dias and J. Leitão, "Wall position and thickness estimation from sequences of echocardiographic images," *IEEE Trans. Med. Imag.*, vol. 15, no. 1, pp. 25–38, Feb. 1996.
[7] M. Figueiredo, J. Leitão, and A. K. Jain, "Adaptive b-splines and boundary estimation," in *IEEE Computer Society Conf. Computer Vision and Pattern Recognition*, Jun. 1997, pp. 724–729.
[8] A. Klein, F. Lee, and A. Amini, "Quantitative coronary angiography with deformable spline models," *IEEE Trans. Med. Imag.*, vol. 16, no. 5, pp. 468–482, Oct. 1997.
[9] O. Germain and P. Réfrégier, "Optimal snake-based segmentation of a random luminance target on a spatially disjoint background," *Opt. Lett.*, vol. 21, no. 22, pp. 1845–1847, 1996.
[10] C. Chesnaud, P. Réfrégier, and V. Boulet, "Statistical region snake-based segmentation adapted to different physical noise models," *IEEE Trans. Pattern Anal. Mach. Intell.*, vol. 21, no. 11, pp. 1145–1157, Nov. 1999.
[11] S. C. Zhu and A. Yuille, "Region competition: Unifying snakes, region growing, and Bayes/MDL for multiband image segmentation," *IEEE Trans. Pattern Anal. Mach. Intell.*, vol. 18, no. 9, pp. 884–900, Sep. 1996.
[12] N. Paragios and R. Deriche, "Geodesic active regions: A new paradigm to deal with frame partition problems in computer vision," *J. Vis. Commun. Image Represent.*, vol. 13, no. 1/2, pp. 249–268, 2002.
[13] J. Rissanen, *Stochastic Complexity in Statistical Inquiry, Series in Computer Science*, vol. 15, 1989, Singapore: World Scientific.
[14] M. Figueiredo, J. Leitão, and A. K. Jain, "Unsupervised contour representation and estimation using B-splines and a minimum description length criterion," *IEEE Trans. Image Process.*, vol. 9, no. 6, pp. 1075–1087, Jun. 2000.
[15] O. Ruch and P. Réfrégier, "Minimal-complexity segmentation with a polygonal snake adapted to different optical noise models," *Opt. Lett.*, vol. 26, no. 13, pp. 977–979, 2001.
[16] P. Martin, P. Réfrégier, F. Goudail, and F. Guérault, "Influence of the noise model on level set active contour segmentation," *IEEE Trans. Pattern Anal. Mach. Intell.*, vol. 26, no. 6, pp. 799–803, Jun. 2004.
[17] N. Paragios and R. Deriche, "Coupled geodesic active regions for image segmentation: A level set approach," in *Proc. European Conf. Computer Vision*, Dublin, Ireland, Jun. 2000, pp. 224–240.
[18] ——, "Geodesic active regions and level set methods for supervised texture segmentation," *Int. J. Comput. Vis.*, vol. 46, no. 3, p. 223, 2002.
[19] J. Kim, J. W. Fisher, A. Yezzi, M. Cetin, and A. S. Willsky, "Nonparametric methods for image segmentation using information theory and curve evolution," in *Proc. IEEE Int. Conf. Image Processing*, Rochester, NY, Sep. 2002, vol. 3, pp. 797–800.
[20] A. Herbulot, S. Jehan-Besson, M. Barlaud, and G. Aubert, "Shape gradient for image segmentation using information theory," in *Proc. IEEE Int. Conf. Acoustics, Speech, and Signal Processing*, Montreal, QC, Canada, May 2004, vol. 3, pp. 21–24.
[21] E. Parzen, "On estimation of a probability density function and mode," *Ann. Math. Statist.*, vol. 33, pp. 1065–1076, 1962.
[22] S. P. Awate, T. Tasdizen, and R. T. Whitaker, Nonparametric Statistics of Image Neighborhoods for Unsupervised Texture Segmentation School Comput., Univ. Utah, 2005, Tech. Rep. UUCS-05-008.
[23] T. M. Cover and J. A. Thomas, *Elements of Information Theory*. New York: Wiley, 1991.
[24] A. El Matouat and M. Hallin, *Order Selection, Stochastic Complexity and Kullback-Leibler Information*. New York: Springer Verlag, 1996, In Memory of E. J. Hannan, pp. 291–299.
[25] A. Dervieux and F. Thomasset, W. Reynolds and R. W. MacCormack, Eds., "Multifluid incompressible flows by a finite elementmethod," in *Proc. 7th Int. Conf. Numerical Methods in Fluid Dynamics*, 1981, vol. 141, Lecture Notes in Physics, pp. 158–163.
[26] S. Osher and J. A. Sethian, "Fronts propagating with curvature dependent speed: Algorithms based on Hamilton-Jacobi formulation," *J. Computat. Phys.*, vol. 79, pp. 12–49, 1988.
[27] J. A. Sethian, "Numerical algorithms for propagating interfaces: Hamilton-Jacobi equations and conservation laws," *J. Different. Geom.*, vol. 31, pp. 131–161, 1990.
[28] V. Caselles, R. Kimmel, and G. Sapiro, "Geodesic active contours," *Int. J. Comput. Vis.*, vol. 22, no. 1, pp. 61–79, 1997.
[29] N. Paragios and R. Deriche, "Geodesic active contours and level sets for the detection and tracking of moving objects," *IEEE Trans. Pattern Anal. Mach. Intell.*, vol. 22, no. 3, pp. 266–280, Mar. 2000.
[30] T. F. Chan and L. A. Vese, "Active contours without edges," *IEEE Trans. Image Process.*, vol. 10, no. 2, pp. 266–277, Feb. 2001.
[31] S. Jehan-Besson, M. Barlaud, and G. Aubert, "Dream2s : Deformable regions driven by an Eulerian accurate minimization method for image and video segmentation," *Int. J. Comput. Vis.*, vol. 53, pp. 45–70, 2003.
[32] F. Galland and P. Réfrégier, "Information theory-based snake adapted to multi-region objects with different noise models," *Opt. Lett.*, vol. 29, no. 14, pp. 1611–1614, 2004.
[33] H. K. Zhao, T. F. Chan, B. Merriman, and S. Osher, "A variational level set approach to multiphase motion," *J. Comp. Phys.*, vol. 127, pp. 179–195, 1996.
[34] L. A. Vese and T. Chan, "A multiphase level set framework for image segmentation using the Mumford and Shah model," *Int. J. Comput. Vis.*, vol. 50, no. 3, pp. 271–293, 2002.
[35] D. L. Chopp, "Computing minimal surfaces via level set curvature flow," *J. Comput. Phys.*, vol. 106, pp. 77–91, 1993.

Authorized licensed use limited to: Pierre Borgnat. Downloaded on February 27, 2009 at 04:51 from IEEE Xplore. Restrictions apply.

[36] F. Goudail, P. Réfrégier, and G. Delyon, "Bhattacharyya distance as a contrast parameter for statistical processing of noisy optical images," *J. Opt. Soc. Amer. A*, vol. 21, no. 7, pp. 1231–1240, 2004.

[37] J. W. Goodman, "Laser speckle and related phenomena," in *Statistical Properties of Laser Speckle Patterns*. Heidelberg, Germany: Springer-Verlag, 1975, vol. 9, Topics in Applied Physics, pp. 9–75.

[38] A. K. Jain*, Fundamentals of Digital Image Processing*. Englewood Cliffs, NJ: Prentice-Hall, 1989, Information and System Sciences Series.

[39] S. J. Sangwine and R. E. N. Horne, "Representations of colour images in different colour spaces," in *The Colour Image Processing Handbook*. London, U.K.: Chapman & Hall, 1998, pp. 76–82.

[40] D. Martin, C. Fowlkes, D. Tal, and J. Malik, "A database of human segmented natural images and its application to evaluating segmentation algorithms and measuring ecological statistics," in *Proc. 8th Int. Conf. Computer Vision*, Jul. 2001, vol. 2, pp. 416–423.

Pascal Martin graduated from Ecole Nationale Supérieure d'Electronique et de Radioélectricité de Grenoble (ENSERG), Grenoble, France, in 2002. He is currently pursuing the Ph.D. degree in the Physique and Image Processing Laboratory, Fresnel Institut (UMR CNRS 6133), Marseille, France, and Simag Développement, Marseille.

His main research interests include image segmentation and statistical techniques.

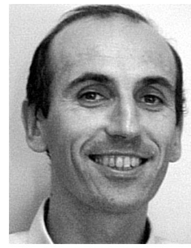

Philippe Réfrégier graduated from Ecole Supérieure de Physique et Chimie Industrielles de la ville de Paris, Paris, France, in 1984, and received the Ph.D. degree in solid-state physics from the University of Paris Orsay, Orsay, France, in 1987.

He is a Full Professor of Signal Processing at Fresnel Institute UMR CNRS 6133, Ecole Généraliste d'Ingénieurs de Marseille, Marseille, France. From 1987 to 1994, he was a member of the Laboratoire Central de Recherches of Thomson-CSF, Orsay. His present research interests include digital image processing and statistical optics. He is the author or editor of several books and proceedings and of about 100 refereed articles in international scientific journals. He has organized and participated in several international conferences.

Frédéric Galland graduated from the Ecole Nationale Supérieure de Physique de Marseille (ENSPM), Marseille, France, in 2001, and received the Ph.D. degree in image processing from the University Paul Cézanne, Marseille, in 2004.

He is currently a Scientific Researcher with CNRS, Fresnel Institut (UMR CNRS 6133), Marseille. His main research interests include image segmentation, synthetic aperture radar image processing, and statistical techniques.

Frédéric Guérault received the Ph.D. degree in image processing from the University of Marseille III, Marseille, France, in 1999.

He was a Postdoctoral Associate in the area of medical image analysis at Creatis, Lyon, France, in 1999 and was then with ONERA, Paris, France, in 2000. Since 2001, he has been the Director of the R&D Department of Simag Développement, Marseille. His research interests are in the areas of computer vision, image processing, and man-machine interfaces.

Authorized licensed use limited to: Pierre Borgnat. Downloaded on February 27, 2009 at 04:51 from IEEE Xplore. Restrictions apply.